3 A precision determination of the $\pi^+\to e^+\nu$ branching ratio

P. Robmann, T. Sakhelashvili, A. van der Schaaf, S. Scheu, and U. Straumann

in collaboration with: Department of Physics, University of Virginia, Charlottesville, USA; Institute for Nuclear Studies, Swierk, Poland; JINR, Dubna, Russia; Paul Scherrer Institut, Villigen, Switzerland and Rudjer Boškoviá Intitute, Zagreb, Croatia

(PEN Collaboration)

3.1 Lepton universality

Lepton universality postulates that the interactions of leptons do not explicitely depend on lepton family number other than through their different masses and mixings. The concept can be generalized to include the quarks. Whereas there is little doubt about the universality of electric charge (*i.e.* the coupling strength to photons) there are scenarios outside the Standard Model (SM) in which lepton universality is violated in the interactions with W and Z bosons.

Allowing for universality violations one can generalize the $V-A$ charged current weak interaction of leptons to [4]:

$$\mathcal{L} = \sum_{l=e,\mu,\tau} \frac{g_l}{\sqrt{2}} W_\mu \overline{\nu}_l \gamma^\mu \left(\frac{1-\gamma_5}{2}\right) l + \text{h.c.} \qquad (3.1)$$

Violations may also have their origin in non-SM contributions to the transition amplitudes. Such apparent violations of lepton universality have been discussed in the literature for various particle decays:

- in W, Z and π decay resulting from R-parity violating extensions to the MSSM (1; 2),
- in W decay resulting from charged Higgs bosons (3),
- in π decay resulting from box diagrams involving non-degenerate sleptons (4),
- in K decay resulting from LFV contributions in SUSY (5),
- in Υ decay resulting from a light Higgs boson (6),
- in π and K decay from scalar interactions (7), enhanced by the strong chiral suppression of the SM amplitude for decays into $e\overline{\nu}_e$. Since these contributions result in interference terms with the SM amplitude the deviations scale with the mass M of the exchange particle like $1/M^2$ rather than $1/M^4$ as may be expected naively.

Experimental limits have recently been compiled by Loinaz *et al.* (8). Results are shown in Table 3.1.

3.2 $\Gamma_{\pi\to e\overline{\nu}}/\Gamma_{\pi\to\mu\overline{\nu}}$

In lowest order (tree level) the decay width of $\pi\to l\overline{\nu}_l$ ($l=e,\mu$) is given by:

$$\Gamma^{\text{tree}}_{\pi\to l\overline{\nu}_l} = \frac{g_l^2 g_{ud}^2 V_{ud}^2}{256\pi}\frac{f_\pi^2}{M_W^4} m_l^2 m_\pi \left(1-\frac{m_l^2}{m_\pi^2}\right)^2 \quad . \qquad (3.2)$$

By taking the branching ratio $R_{e/\mu} \equiv \Gamma_{\pi\to e\overline{\nu}}/\Gamma_{\pi\to\mu\overline{\nu}}$ the factors affected by hadronic uncertainties cancel. Radiative corrections lower the result by 3.74(3)% (9) when assuming that final states with additional photons are included.

---

[4] Still more general violations lead to deviations from the $1-\gamma_5$ structure of the weak interaction.

Table 3.1: Limits on lepton universality from various processes. Violations may affect the various tests differently so which constraint is best depends on the mechanism. Hypothetical non V-A contributions, for example, would lead to larger effects in decay modes with stronger helicity suppression such as $\pi \to e\nu$ and $K \to e\nu$. Adapted from Ref. [8].

decay mode	constraint	
$W \to e\,\overline{\nu}_e$	$(g_\mu/g_e)_W = 0.999$	$\pm\, 0.011$
$W \to \mu\,\overline{\nu}_\mu$	$(g_\tau/g_e)_W = 1.029$	$\pm\, 0.014$
$W \to \tau\,\overline{\nu}_\tau$		
$\mu \to e\,\overline{\nu}_e\,\nu_\mu$	$(g_\mu/g_e)_\tau = 0.9999$	$\pm\, 0.0021$
$\tau \to e\,\overline{\nu}_e\,\nu_\tau$	$(g_\tau/g_e)_{\tau\mu} = 1.0004$	$\pm\, 0.0022$
$\tau \to \mu\,\overline{\nu}_\mu\,\nu_\tau$		
$\pi \to e\,\overline{\nu}_e$	$(g_\mu/g_e)_\pi = 1.0021$	$\pm\, 0.0016$
$\pi \to \mu\,\overline{\nu}_\mu$	$(g_\tau/g_e)_{\tau\pi} = 1.0030$	$\pm\, 0.0034$
$\tau \to \pi\,\nu_\tau$		
$K \to e\,\overline{\nu}_e$	$(g_\mu/g_e)_K = 1.024$	$\pm\, 0.020$
$K \to \mu\,\overline{\nu}_\mu$	$(g_\tau/g_\mu)_{K\tau} = 0.979$	$\pm\, 0.017$
$\tau \to K\,\overline{\nu}_\tau$		

This leads to the theoretical prediction:

$$R_{e/\mu}^{\mathrm{theor.}} = (g_e/g_\mu)^2 \times 1.2354(2) \cdot 10^{-4} \quad . \tag{3.3}$$

Two experiments (10; 11) contribute to the present world average for the measured value:

$$R_{e/\mu}^{exp.} = 1.231(4) \times 10^{-4} \quad . \tag{3.4}$$

As a result μe universality has been tested at the level: $(g_\mu/g_e)_\pi$=1.0021(16) (see Table 3.1).

3.3 Measurement principles

Measurements of $R_{e/\mu}$ are based on the analysis of e^+ energy and time delay with respect to the stopping π^+. The decay $\pi \to e\nu$ is characterized by $E_{e^+} = 0.5 m_\pi c^2 = 69.8$ MeV and an exponential time distribution following the pion life time τ_π=26 ns. In the case of the $\pi \to \mu\nu$ decay the 4 MeV muons which have a range of about 1.4 mm in plastic scintillator can be kept inside the target and are monitored by the observation of the subsequent decay $\mu \to e\nu\overline{\nu}$ which is characterized by $E_{e^+} < 0.5 m_\mu c^2 = 52.8$ MeV and a time distribution which first grows according to the pion life time and then falls with the muon life time.

A major systematic error is introduced by uncertainties in the low-energy tail of the $\pi \to e\nu(\gamma)$ energy spectrum in the region below $0.5 m_\mu c^2$. This tail fraction typically amounts to ≈1 % . The low-energy tail can be studied by suppressing the $\pi \to \mu \to e$ chain by the selection of early decays and by vetoing events in which the muon is observed in the target signal. Suppression factors of typically 10^{-5} have been obtained. A study of this region is also interesting since it might reveal the signal from a heavy sterile neutrino (12).

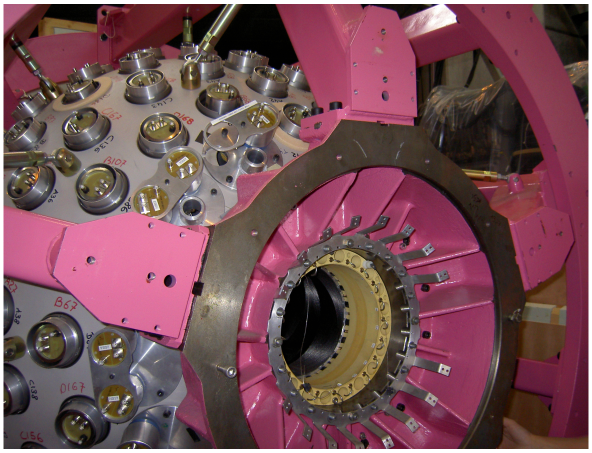

Figure 3.1: The PEN CsI calorimeter before installation of the cylindrical tracking detectors and beam counters shown in Fig. 3.2.

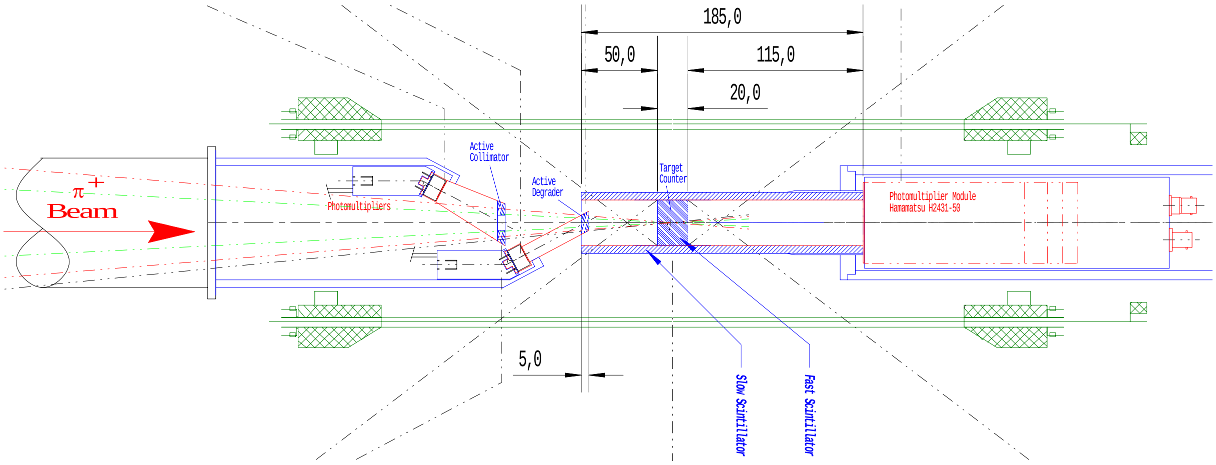

Figure 3.2: y - z **view of the innermost MWPC (in green) and three of the four beam counters (in blue). A fourth detector situated in an intermediate focus a few meters upstream is used to measure particle velocities which helps to suppress muons in the beam and to calculate the pion momentum on an event-by-event basis.**

3.4 Status of PEN

Both at PSI (13) and at TRIUMF (16) proposals for new $R_{e/\mu}$ measurements have been accepted. At PSI the 3π sr CsI calorimeter built for a determination of the $\pi^+ \to \pi^0 e^+ \nu$ branching ratio (see Fig. 3.1) is being used. The setup was also used for the most complete studies of the radiative decays $\pi \to e\nu\gamma$ (14) and $\mu \to e\nu\overline{\nu}\gamma$ (15) done so far.

Large samples of $\pi \to e\nu$ decays have been recorded parasitically in the past which were used as normalization for $\pi^+ \to \pi^0 e^+ \nu$ with an accuracy of $< 0.3\%$, *i.e.* the level of the present experimental uncertainty of $R_{e/\mu}$. Based on this experience an improvement in precision for $R_{e/\mu}$ by almost an order of magnitude is expected.

Our institute supplied new beam counters optimized for the specific requirements of these measurements (Fig. 3.2) *i.e.* optimal time, energy and double-pulse resolutions. The signals from these fast scintillating detectors are recorded with wave-form digitizers allowing for optimal off-line reconstruction of the complex target information containing two or three overlapping signals (see Fig. 3.3).

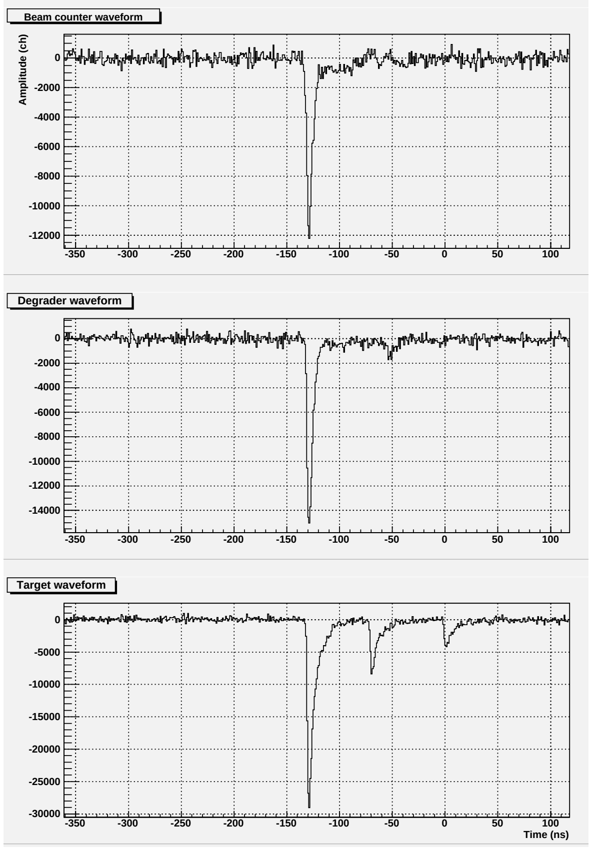

Figure 3.3: Beam-counter wave forms for the event of a π^+ **stopping in the active target followed by the decay sequence** $\pi \to \mu\overline{\nu}$, $\mu \to e\nu\overline{\nu}$. **The sampling frequency is 2 GHz.**

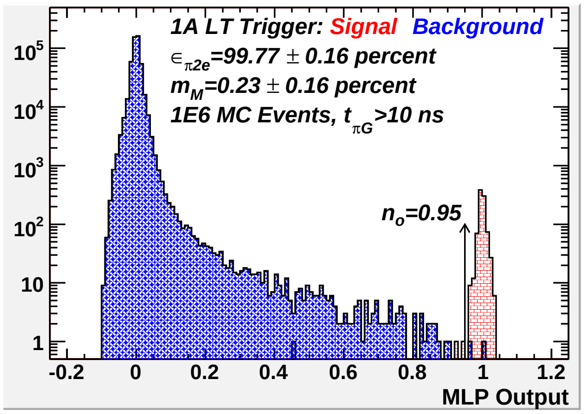

Figure 3.4: Separation of $\pi\rightarrow e\overline{\nu}$ and $\pi\rightarrow\mu\overline{\nu}$ events using a multi-layer perceptron (MLP) artificial neural network.

As mentioned above the separation of $\pi \rightarrow e\nu(\gamma)$ from $\pi \rightarrow \mu\nu(\gamma)$ is based on the analysis of many pieces of information. As discussed in some detail in Sec. 5 for the separation of single photons from π^0 decays various methods are available. Figure 3.4 shows as an example the separation obtained with an artificial neural network.

Presently we are replacing the plastic hodoscope situated between the tracking detectors detectors and the CsI calorimeter. First tests have shown that the light yield will increase by more than an order of magnitude which will guarantee both the very high positron detection efficiency and the sub-nanosecond time resolution required for this experiment. Starting early September we hope to take data which should lead to a first significant improvement in $R_{e/\mu}$.

[1] O. Lebedev, W. Loinaz and T. Takeuchi, Phys. Rev. D **61** (2000) 115005.

[2] M. J. Ramsey-Musolf, Phys. Rev. D **62** (2000).

[3] J. h. Park, JHEP **0610** (2006) 077.

[4] M. J. Ramsey-Musolf and S. Su, "Low energy precision test of supersymmetry," arXiv:hep-ph/0612057.

[5] A. Masiero, P. Paradisi and R. Petronzio, Phys. Rev. D **74** (2006) 011701.

[6] M. A. Sanchis-Lozano, Contributed paper to the Workshop on B-Factories and New Measurements, September 13-14, 2006, KEK, arXiv:hep-ph/0610046.

[7] B.A. Campbell and D.W. Maybury, Nucl. Phys .B709, 419 (2005).

[8] W. Loinaz, N. Okamura, S. Rayyan, T. Takeuchi and L. C. R. Wijewardhana, Phys. Rev. D **70** (2004) 113004.

[9] M. Finkemeier, Phys. Lett. B **387** (1996) 391.

[10] G. Czapek et al., Phys. Rev. Lett. **70** (1993) 17.

[11] D. I. Britton et al., Phys. Rev. Lett. **68** (1992) 3000.

[12] Smirnov, and R. Funchal, Phys.Rev.D74:013001 (2006).

[13] PEN Collaboration, PSI experiment R-05-01, D. Pocanic and A. van der Schaaf, spokespersons.

[14] M. A. Bychkov, Ph.D. thesis, University of Virginia, (2005), unpublished.

[15] B. A. VanDevender, Ph.D. thesis, University of Virginia,(2005), unpublished.

[16] PIENU Collaboration, TRIUMF experiment 1072, D. Bryman and T. Numao, spokespersons.